Supplemental material

Liu et al., https://doi.org/10.1084/jem.20180749

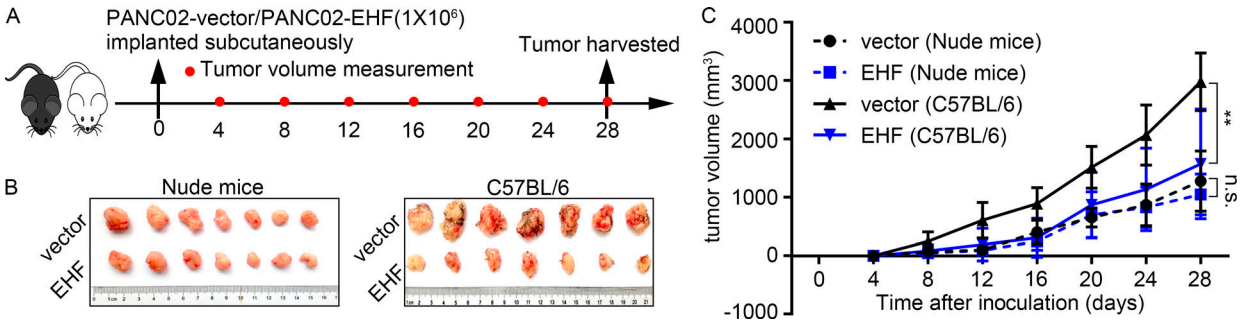

Figure S1. **Tumoral EHF inhibits tumor growth significantly in immunocompetent mice. (A)** Immunocompetent C57BL/6 mice and immunocompromised BALB/C nude mice were subcutaneously inoculated with PANC02-vector or PANC02-EHF. Tumor volumes were measured every 4 d after inoculation and harvested on day 28. **(B)** Tumors at the end point of the experiment are shown (left, BALB/C nude mice; right, C57BL/6 mice). **(C)** Tumor growth curves of the four groups. All mouse experiments were repeated three times independently, using seven mice per experimental group. Representative data are shown. Data are presented as mean ± SD. Repeated measure two-way ANOVA (time × tumor volume) and post hoc analysis were used for test mouse tumor growth between groups. **, $P < 0.01$; n.s., not significant.

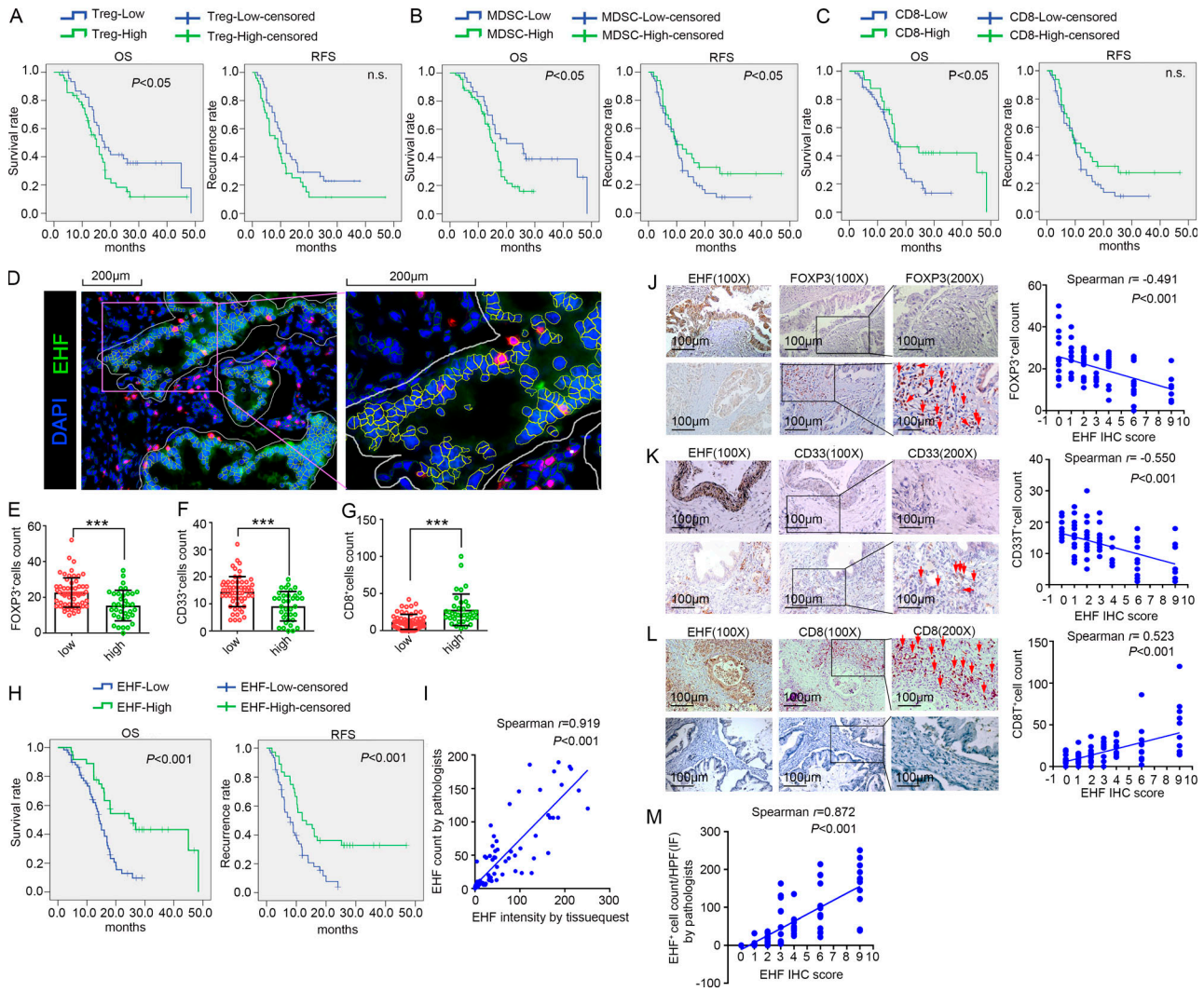

Figure S2. **The correlation of tumoral EHF expression with tumor-infiltrating immune cells content in human PDAC tissue. (A–C)** Prognostic significance of tumor-infiltrating T reg cells (A), MDSCs (B), and CD8⁺ T cells (C) for OS (left) and RFS (right) in a series of 96 cases of PDAC. Kaplan–Meier OS and RFS for different levels of CD8⁺ T cell infiltration, T reg cell accumulation, and MDSC accumulation are shown based on log-rank statistic test. n.s., not significant. The data were based on IF. **(D)** The objective evaluation method for EHF. Mean EHF intensity was quantified by using TissueQuest software 6.0. Tumor areas were manually outlined to exclude stromal nuclei. DAPI was used to identify nuclei. **(E–G)** The percentage of tumor-infiltrating Foxp3⁺ cells, CD33⁺ cells, and CD8⁺ cells were compared between the high-EHF group and low-EHF group. Nonpaired Student's *t* test was used as statistical analysis; *n* = 96; ***, P < 0.001. **(H)** Kaplan–Meier OS (left) and RFS (right) for different levels of EHF based on the log-rank statistic test (P < 0.001). **(I)** Spearman correlation analysis between EHF intensity evaluated by software and EHF-positive cell count/HPF evaluated by pathologists. P < 0.001 by Spearman correlation analysis. **(J–L)** Four consecutive sets of PDAC tissues were stained with FOXP3, CD33, CD8, and EHF by IHC. The densities of FOXP3⁺ cells (G), CD33⁺ cells (H) and CD8⁺ cells (I) were quantified. One example of the 96 cases is shown. The arrows indicate tumor infiltration of Foxp3⁺ T reg cells, CD33⁺ myeloid cells, and CD8⁺ T cells, respectively. Bars, 100 μm. Spearman correlation analyses were performed between tumor-infiltrating immune cells and EHF IHC score (T reg cells, J, right; MDSCs, K, right; CD8⁺ T cells, L, right). **(M)** Spearman correlation analysis between EHF IF result (EHF-positive cell count/HPC) and EHF IHC score evaluated by pathologists. P < 0.001 by Spearman correlation analysis.

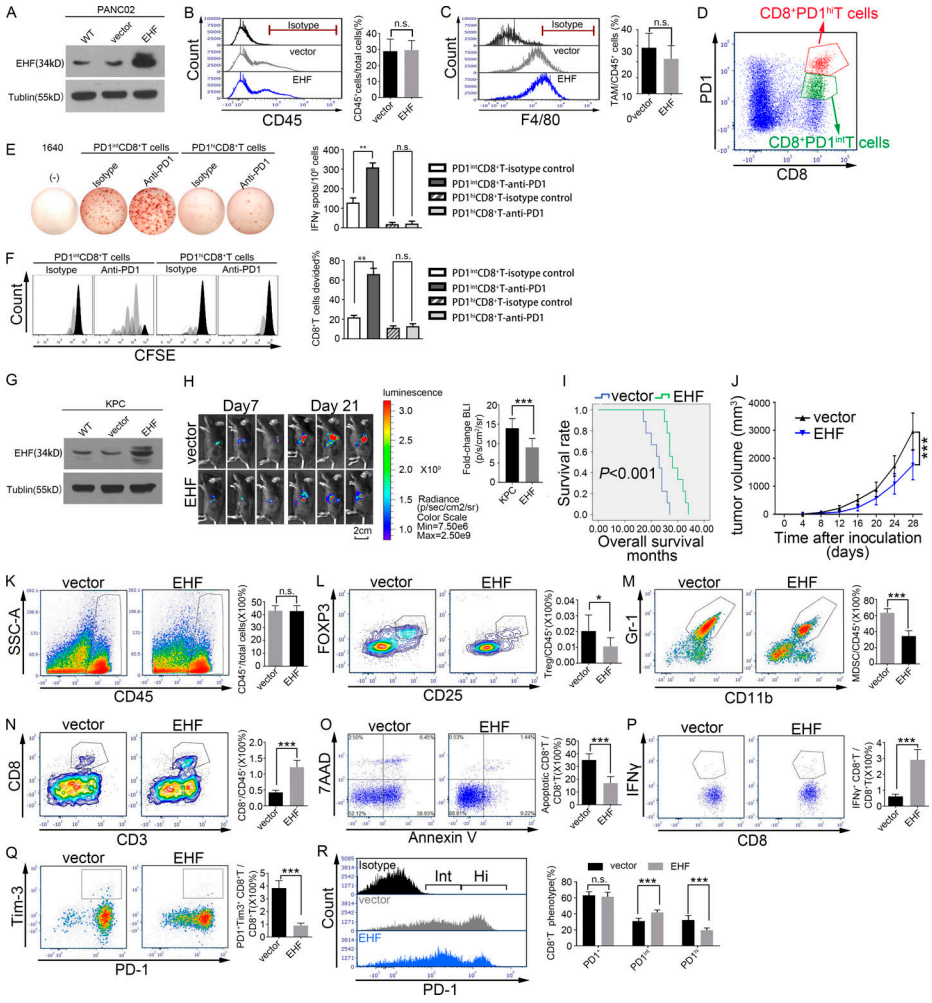

Figure S3. **Results from an additional mouse model using KPC-vector and KPC-EHF cell lines. (A)** EHF protein expression analysis of PANC02, PANC02-vector, and PANC02-EHF by Western blotting. Experiments were repeated three times. Representative data are shown. **(B)** Representative histogram (left) and statistical analysis (right) of the percentage of tumor-infiltrating CD45$^+$ cells. **(C)** Representative histogram (left) and statistical analysis (right) of tumor-infiltrating TAMs using CD45, CD11b, and F4/80 staining. CD45, CD11b double-positive cells were gated. CD45$^+$CD11b$^+$F4/80$^+$ TAM (%) = CD45$^+$Gr-1$^+$CD11b$^+$ TAM cell count/CD45$^+$cell count. **(D–F)** Different response of tumor-infiltrating CD8$^+$PD1^{int} T cells and CD8$^+$PD1^{hi} T cells to PD1 blockage therapy. **(D)** The isolation scheme for CD8$^+$PD1^{int} T cells and CD8$^+$PD1^{hi} T cells by flow cytometry. **(E)** The capacity of tumor-infiltrating CD8$^+$PD1^{int} T cells and CD8$^+$PD1^{hi} T cells to produce IFNγ upon anti-CD3 stimulation in the presence of antibodies blocking PD1 or isotype control. Representative IFNγ-ELISPOT plots (left) and statistical analysis (right) are shown. **(F)** Representative histogram (left) and statistical analysis (right) of CD8$^+$PD1^{int} T cells and CD8$^+$PD1^{hi} T cells division proportion following anti-CD3 stimulation without or with anti-PD-1 therapy. The in vitro functional restoration assay and TIL sorting (D–F) were repeated three times independently. Representative data are shown. Paired Student's *t* test was used for statistical analysis; **, P < 0.01; n.s. not significant. **(G)** EHF protein expression analysis of KPC, KPC-vector, and KPC-EHF by Western blotting. Experiments were repeated three times. Representative data are shown. **(H)** C57BL/6 mice were orthotopically injected with 5 × 10^5 luciferase-expressing KPC-vector cells or luciferase-expressing KPC-EHF cells in Matrigel. Tumor growth was assessed by BLI at days 7 and 21. Three representative bioluminescent images of the two groups on days 7 and 21 after tumor implantation are shown (left). Statistical analysis of the fold change of BLI on day 21 to BLI on day 7 (right); ***, P < 0.001 by nonpaired Student's *t* test (*n* = 9 per group). **(I)** C57BL/6 mice were orthotopically injected with 1 × 10^6 luciferase-expressing KPC-vector cells or luciferase-expressing KPC-EHF cells in Matrigel. Kaplan–Meier survival curves with log-rank test for significance between KPC-vector and KPC-EHF, P < 0.001 (*n* = 9 per group). **(J)** C57BL/6 mice were subcutaneously inoculated with 1 × 10^6 KPC-vector or KPC-EHF. Tumor volumes were measured every 4 d after inoculation until day 28. The experiments were repeated three times independently, using seven mice per experimental group. Repeated measure two-way ANOVA (time × tumor volume) and post hoc analysis were used for test mouse tumor growth between KPC-vector and KPC-EHF. ***, P < 0.001. **(K–R)** Immunocompetent C57BL/6 mice were subcutaneously inoculated with 5 × 10^5 KPC-vector or KPC-EHF. Mice were sacrificed when tumor volumes reached a threshold of 1,500 mm^3. **(K)** Representative plots (left) and statistical analysis (right) of the percentage of tumor-infiltrating CD45$^+$ cells. **(L–N)** Results for CD4$^+$CD25$^+$FOXP3$^+$ T reg cells, CD45$^+$CD11b$^+$Gr-1$^+$ MDSCs and CD3$^+$CD8$^+$ T cells as frequencies of CD45$^+$ leukocytes. Representative plots (left) and statistical analysis (right) of the frequency of tumor-infiltrating T reg cells (L), MDSCs (M), and CD3$^+$CD8$^+$ T cells (N) are shown. **(O–Q)** Representative plots (left) and statistical analysis (right) of the frequency of tumor-infiltrating CD8$^+$ T cell apoptosis (O), CD8$^+$IFNγ$^+$ T cells (P), and CD8$^+$ T cell exhaustion (PD1$^+$Tim3$^+$CD8$^+$ T; Q). CD8$^+$ T cells were gated. The percentage calculations used CD8$^+$ T cell count as the denominator. **(R)** Representative histogram (left) and statistical analysis (right) on the frequency of PD1$^+$CD8$^+$ T (left), PD1^{int}CD8$^+$ T (middle), and PD1^{hi}CD8$^+$ T (right) cells. CD8$^+$ T cells were gated. The percentage calculations used CD8$^+$ T cells count as the denominator. All mouse experiments were repeated three times independently, using seven mice per experimental group in subcutaneous tumor model and nine mice per experimental group in orthotopic tumor model. Data are presented as mean ± SD. Nonpaired Student's *t* test was used as statistical analysis (K–R); *, P < 0.01; ***, P < 0.001; n.s., not significant.

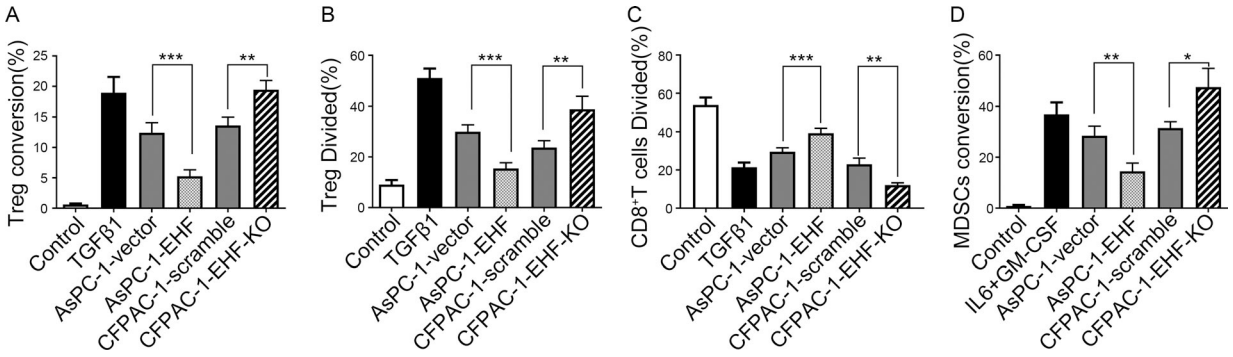

Figure S4. **Data from another two pancreatic cells lines for in vitro coculture experiments. (A)** Percentage of T reg conversion from $CD4^+CD25^-$ T cells. T reg cell conversion induced by AsPC-1-EHF cells relative to AsPC-1-vector and T reg cell conversion induced by CFPAC-1-EHF-KD cells relative to CFPAC-1-scramble are shown. **(B)** Statistical analysis of the percentage of T reg cell division. T reg cell divided induced by AsPC-1-EHF cells relative to AsPC-1-vector and T reg cell conversion induced by CFPAC-1-EHF-KD cells relative to CFPAC-1-scramble are shown. **(C)** T reg suppression assay by comparing the percentage of $CD8^+$ T cells division cocultured with AsPC-1-EHF (CFPAC-1-EHF-KD)–generated T reg cells and AsPC-1-vector (CFPAC-1-scramble)–generated T reg cells. Statistical analysis of the proportion of CFSE-labeled $CD8^+$ T cell division. **(D)** The frequency of $CD11b^+CD33^+$ cells among HLA-DR^- cells was quantified in the bar graph. Human PBMCs were cultured in vitro under different conditions (negative control, RPMI 1640; positive control, IL6 and GM-CSF; experimental group, AsPC-1-vector, AsPC-1-EHF, CFPAC-1-scramble, and CFPAC-1-EHF-KD) and analyzed on day 6 to determine MDSC marker expression by flow cytometry. All the coculture experiments were repeated five times independently. Data are presented as mean ± SD. Paired Student's *t* test was used for statistical analyses; *, $P < 0.05$; **, $P < 0.01$; ***, $P < 0.001$.

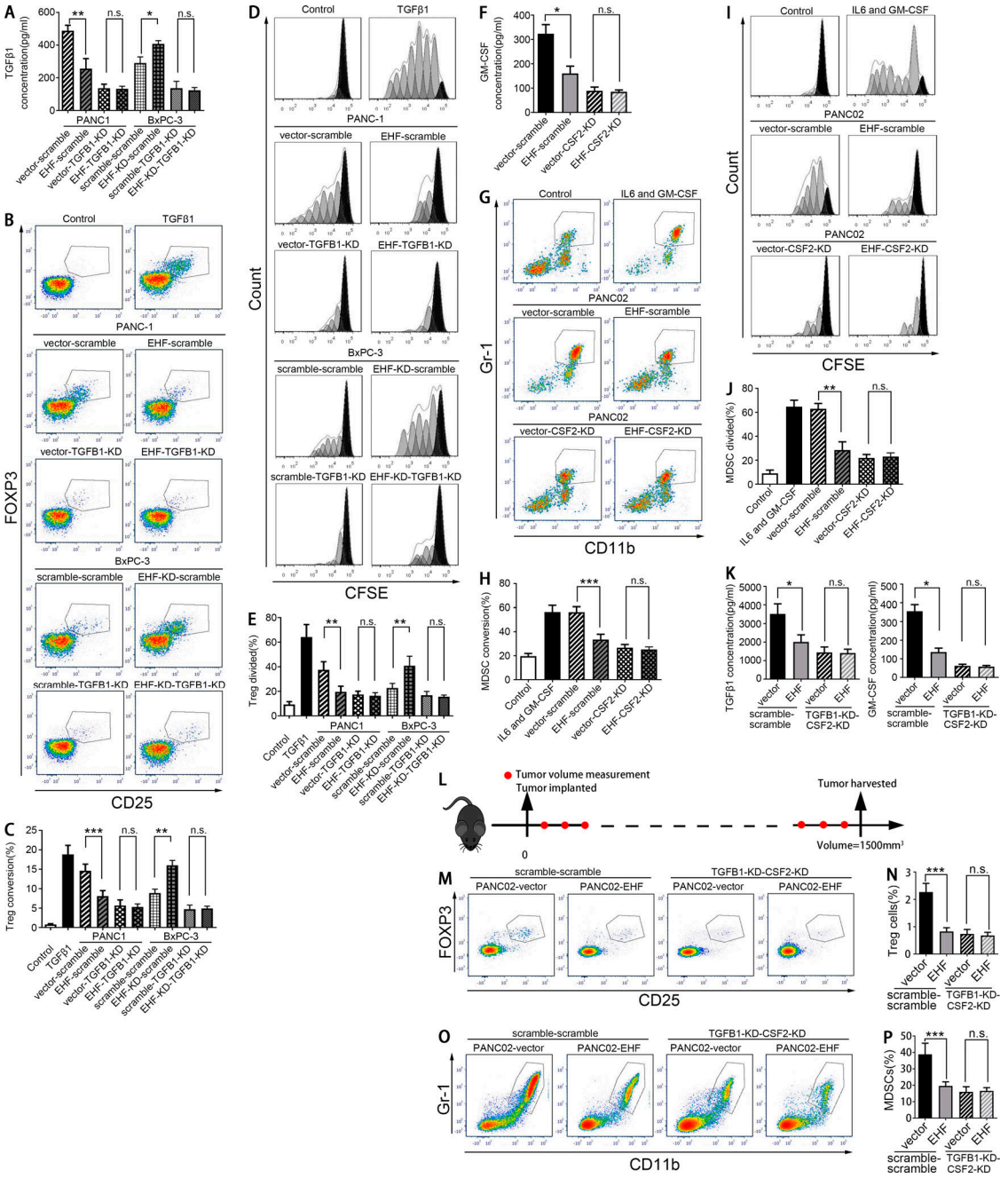

Figure S5. **In vitro and in vivo blocking experiments using cell lines with genetic knockdown of TGF-B1 and CSF2. (A)** TGFβ1 expression analysis by ELISA in PANC-1-vector-scramble, PANC-1-vector-TGFB1-KD, PANC-1-EHF-scramble, PANC-1-EHF-TGFB1-KD, BxPC3-scramble-scramble, BxPC3-scramble-TGFB1-KD, BxPC3-EHF-KD-scramble, and BxPC3-EHF-KD-TGFB1-KD. **(B and C)** Representative plots (B) and statistical analysis (C) of $CD4^+CD25^-$ T cells to T reg conversion induced by indicated cell lines. **(D and E)** Representative plots (D) and statistical analysis (E) of T reg cell proliferation induced by indicated cell lines. TGFβ1 was used as a positive control, and RPMI 1640 was used as negative control. **(F)** GM-CSF expression analysis by ELISA in PANC02-vector-scramble, PANC02-EHF-scramble, PANC02-vector-CSF2-KD, and PANC02-EHF-CSF2-KD. **(G and H)** Representative plots (G) and statistical analysis (H) of MDSC conversion induced by indicated cell lines. **(I and J)** Representative plots (I) and statistical analysis (J) of MDSCs proliferation induced by indicated cell lines. IL-6 and GM-CSF were used as a positive control, and RPMI 1640 was used as negative control. **(K)** TGFβ1 (left) and GM-CSF (right) expression analysis by ELISA in PANC02-vector-scramble-scramble, PANC02-EHF-scramble-scramble, PANC02-vector-TGFB1-KD-CSF2-KD, and PANC02-EHF-TGFB1-KD-CSF2-KD. **(L)** Immunocompetent C57BL/6 mice were subcutaneously inoculated with PANC02-vector-scramble-scramble, PANC02-EHF-scramble-scramble, PANC02-vector-TGFB1-KD-CSF2-KD, and PANC02-EHF-TGFB1-KD-CSF2-KD. Mice were sacrificed when tumor volumes reached a threshold of 1,500 mm^3. **(M–P)** Representative dot plots (left) and statistical analysis (right) of the proportion of tumor infiltration T reg cells (M and N) and MDSCs (O and P) in the PANC02-vector-scramble-scramble, PANC02-EHF-scramble-scramble, PANC02-vector-TGFB1-KD-CSF2-KD, and PANC02-EHF-TGFB1-KD-CSF2-KD groups. All the ELISA experiments (A, F, and K) were repeated three times independently. Paired Student's *t* test was used for statistical analysis. All the coculture experiments (B–E and G–J) were repeated five times independently. Paired Student's *t* test was used for statistical analysis. All mouse experiments (M–P) were repeated three times independently, using seven mice per experimental group. Nonpaired Student's *t* test was used for statistical analysis; *, $P < 0.05$; **, $P < 0.01$; ***, $P < 0.001$; n.s., not significant.

Table S1. **Univariate and multivariate Cox proportional hazards analysis of clinicopathological factors for OS and RFS**

Variables	OS		RFS	
	HR (95.0% CI)	P	HR (95.0% CI)	P
Univariate analysis				
Age	0.932 (0.570–1.524)	0.780	0.805 (0.508–1.275)	0.355
Sex	1.398 (0.855–2.287)	0.182	1.335 (0.842–2.114)	0.219
Histological grade	1.772 (1.058–2.969)	0.030[a]	1.621 (1.001–2.627)	0.05
Tumor size	1.133 (0.688–1.868)	0.624	1.058 (0.664–1.684)	0.813
pTNM stage	2.174 (1.153–4.100)	0.016[a]	2.462 (1.363–4.447)	0.003[a]
LN metastasis	1.417 (0.768–2.612)	0.265	1.440 (0.816–2.543)	0.209
EHF expression	0.311 (0.164–0.591)	0.000[a]	0.312 (0.173–0.562)	0.000[a]
CD8	0.561 (0.324–0.972)	0.039[a]	0.676 (0.411–1.114)	0.124
T reg cell	1.742 (1.061–2.862)	0.028[a]	1.520 (0.956–2.417)	0.077
MDSC	1.906 (1.088–3.339)	0.024[a]	1.897 (1.126–3.195)	0.016[a]
Multivariate analysis				
pTNM stage	1.920 (1.004–3.669)	0.049[a]	1.964 (1.078–3.580)	0.027[a]
EHF expression	0.371 (0.193–0.712)	0.003[a]	0.362 (0.200–0.657)	0.001[a]

Data were based on IF assay. Mean intensity of EHF was evaluated by software. Multivariate Cox proportional hazards analysis used backward selection model. Abbreviations: HR, hazard ratio; CI, confidence interval.
[a]Statistically significant ($P < 0.05$).

Table S2. **Correlation of EHF expression to clinicopathological features in PDAC**

Parameters	EHF (*n*)		χ^2	P	Spearman *r*
	Low	High			
Age (yr)					
<60	36	11	0.631	0.427	0.081
≥60	34	15			
Sex					
Male	35	17	1.807	0.179	−0.137
Female	35	9			
Histological grade					
G1, G2	41	22	5.7	0.017[a]	−0.244
G3	29	4			
pTNM stage					
IA, IB	14	11	4.898	0.027[a]	−0.226
IIA, IIB	56	15			
CD8					
≤20/HP	51	12	5.993	0.014[a]	0.250
>20/HP	19	14			
T reg cell					
≤20/HP	26	18	5.864	0.015[a]	−0.247
>20/HP	44	8			
MDSC					
≤10/HP	15	15	11.604	0.001[a]	−0.348
>10/HP	55	11			

Data were based on IF assay. Mean intensity of EHF was evaluated by software. Statistical data on EHF expression in relation to clinic-histopathologic features for surgical PDAC specimens. P values were calculated using the χ^2 test.
[a]Statistically significant ($P < 0.05$).

Table S3. **Univariate and multivariate Cox proportional hazards analysis of clinicopathological factors for OS and RFS**

Variables	OS		RFS	
	HR (95.0% CI)	P	HR (95.0% CI)	P
Univariate analysis				
Age	0.932 (0.570–1.524)	0.780	0.805 (0.508–1.275)	0.355
Sex	1.398 (0.855–2.287)	0.182	1.335 (0.842–2.114)	0.219
Histological grade	1.772 (1.058–2.969)	0.030[a]	1.621 (1.001–2.627)	0.05
Tumor size	1.133 (0.688–1.868)	0.624	1.058 (0.664–1.684)	0.813
pTNM stage	2.174 (1.153–4.100)	0.016[a]	2.462 (1.363–4.447)	0.003[a]
LN metastasis	1.417 (0.768–2.612)	0.265	1.440 (0.816–2.543)	0.209
EHF expression[b]	0.342 (0.184–0.638)	0.001[a]	0.336 (0.189–0.596)	0.000[a]
CD8	0.561 (0.324–0.972)	0.039[a]	0.676 (0.411–1.114)	0.124
T reg cell	1.742 (1.061–2.862)	0.028[a]	1.520 (0.956–2.417)	0.077
MDSC	2.047 (1.156–3.623)	0.014[a]	2.009 (1.183–3.412)	0.010[a]
Multivariate analysis				
pTNM stage	1.937 (1.014–3.702)	0.045[a]	1.975 (1.082–3.606)	0.027[a]
EHF expression	0.411 (0.218–0.775)	0.006[a]	0.392 (0.219–0.702)	0.002[a]

Data were based on IHC assay. Multivariate Cox proportional hazards analysis used backward selection model. Abbreviations: HR, hazard ratio; CI, confidence interval.

[a]Statistically significant ($P < 0.05$).

[b]Here, EHF expression was divided into high-EHF and low-EHF according to the data of EHF-positive cell count/HPF evaluated by IHC. The count of EHF-positive points/HPF by IHC ranged from 0 to 226, mean ± S.D., 40.89 ± 55.51. EHF-positive cells/HPF > 40.89 was considered as high EHF; EHF-positive cells/HPF < 40.89 was considered as low EHF.

Table S4. **Correlation of EHF expression to clinicopathological features in PDAC**

Parameters	EHF (*n*)[a]		χ^2	P	Spearman *r*
	Low	High			
Age (yr)					
<60	36	11	1.015	0.368	0.103
≥60	33	16			
Sex					
Male	34	18	2.364	0.172	−0.157
Female	35	9			
Histological grade					
G1, G2	40	23	6.371	0.016[b]	−0.258
G3	29	4			
pTNM stage					
IA, IB	13	12	6.605	0.018[b]	−0.262
IIA, IIB	56	15			
CD8					
≤20/HP	51	12	7.470	0.009[b]	0.279
>20/HP	18	15			
T reg cell					
≤20/HP	28	19	6.892	0.012[b]	−0.268
>20/HP	41	8			
MDSC					
≤10/HP	13	16	15.037	0.000[b]	−0.396
>10/HP	56	11			

Data were based on IHC assay. Statistical data on EHF expression in relation to clinic-histopathologic features for surgical PDAC specimens. P values were calculated using the χ^2 test.

[a]Here, EHF expression was divided into high-EHF and low-EHF according to the data of EHF-positive cell count/HPF evaluated by IHC. The count of EHF-positive points/HPF by IHC ranged from 0 to 226, mean ± S.D., 40.89 ± 55.51. EHF-positive cells/HPF > 40.89 was considered as high EHF; EHF-positive cells/HPF < 40.89 was considered as low EHF.

[b]Statistically significant ($P < 0.05$).

Table S5. **shRNA sequences for stable knockdown cell lines**

The name of shRNA	Sequence
Human EHF shRNA1 (most efficient)	
Top	5′-ccggGCCAATTGTATCCCTTTCCAACTCGAGTTGGAAAGGGATACAATTGGCttttt-3′
Bottom	5′-attaaaaaGCCAATTGTATCCCTTTCCAACTCGAGTTGGAAAGGGATACAATTGGC-3′
Human EHF shRNA2	
Top	5′-ccggGGGAGTTCATCCGAGACATTCCTCGAGGAATGTCTCGGATGAACTCCCttttt-3′
Bottom	5′-aattaaaaaGGGAGTTCATCCGAGACATTCCTCGAGGAATGTCTCGGATGAACTCCC-3′
Human EHF shRNA3	
Top	5′-ccggAGTCCGCACACAATGTCATTGCTCGAGCAATGACATTGTGTGCGGACttttt-3′
Bottom	5′-aattaaaaaAGTCCGCACACAATGTCATTGCTCGAGCAATGACATTGTGTGCGGAC-3′
Human TGFB1 shRNA1 (most efficient)	
Top	5′-ccggACTGCGGATCTCTGTGTCATTctcgagAATGACACAGAGATCCGCAGTttttt-3′
Bottom	5′-aattaaaaaACTGCGGATCTCTGTGTCATTctcgagAATGACACAGAGATCCGCAGT-3′
Human TGFB1 shRNA2	
Top	5′-ccggCCCGCGTGCTAATGGTGGAAActcgagTTTCCACCATTAGCACGCGGGttttt-3′
Bottom	5′-aattaaaaaCCCGCGTGCTAATGGTGGAAActcgagTTTCCACCATTAGCACGCGGG-3′
Human TGFB1 shRNA3	
Top	5′-ccggCCACAACGAAATCTATGACAActcgagTTGTCATAGATTTCGTTGTGGttttt-3′
Bottom	5′-aattaaaaaCCACAACGAAATCTATGACAActcgagTTGTCATAGATTTCGTTGTGG-3′
Human CSF2 shRNA1 (most efficient)	
Top	5′-ccggCCCAGATTATCACCTTTGAAActcgagTTTCAAAGGTGATAATCTGGGttttt-3′
Bottom	5′-aattaaaaaCCCAGATTATCACCTTTGAAActcgagTTTCAAAGGTGATAATCTGGG-3′
Human CSF2 shRNA2	
Top	5′-ccggGAAGGACTTTCTGCTTGTCATctcgagATGACAAGCAGAAAGTCCTTCttttt-3′
Bottom	5′-aattaaaaaGAAGGACTTTCTGCTTGTCATctcgagATGACAAGCAGAAAGTCCTTC-3′
Human CSF2 shRNA3	
Top	5′-ccggGAAGTCATCTCAGAAATGTTTctcgagAAACATTTCTGAGATGACTTCttttt-3′
Bottom	5′-aattaaaaaGAAGTCATCTCAGAAATGTTTctcgagAAACATTTCTGAGATGACTTC-3′
Murine TGFB1 shRNA1	
Top	5′-cggCGGCAGCTGTACATTGACTTTctcgagAAAGTCAATGTACAGCTGCCGttttt-3′
Bottom	5′-aattaaaaaCGGCAGCTGTACATTGACTTTctcgagAAAGTCAATGTACAGCTGCCG-3′
Murine TGFB1 shRNA2	
Top	5′-ccggGCTCTTGTGACAGCAAAGATActcgagTATCTTTGCTGTCACAAGAGCttttt-3′
Bottom	5′-aattaaaaaGCTCTTGTGACAGCAAAGATActcgagTATCTTTGCTGTCACAAGAGC-3′
Murine TGFB1 shRNA3 (most efficient)	
Top	5′-ccggCGAAGCGGACTACTATGCTAActcgagTTAGCATAGTAGTCCGCTTCGttttt-3′
Bottom	5′-aattaaaaaCGAAGCGGACTACTATGCTAActcgagTTAGCATAGTAGTCCGCTTCG-3′
Murine CSF2 shRNA1 (most efficient)	
Top	5′-ccggAGCCAGCTACTACCAGACATActcgagTATGTCTGGTAGTAGCTGGCTttttt-3′
Bottom	5′-aattaaaaaAGCCAGCTACTACCAGACATActcgagTATGTCTGGTAGTAGCTGGCT-3′
Murine CSF2 shRNA2	
Top	5′-ccggCGTCTCTAACGAGTTCTCCTTctcgagAAGGAGAACTCGTTAGAGACGttttt-3′
Bottom	5′-aattaaaaaCGTCTCTAACGAGTTCTCCTTctcgagAAGGAGAACTCGTTAGAGACG-3′
Murine CSF2 shRNA3	
Top	5′-ccggCGGATTTCATAGACAGCCTTActcgagTAAGGCTGTCTATGAAATCCGttttt-3′

Table S5. **shRNA sequences for stable knockdown cell lines (*Continued*)**

The name of shRNA	Sequence
Bottom	5′-aattaaaaaCGGATTTCATAGACAGCCTTActcgagTAAGGCTGTCTATGAAATCCG-3′

Uppercase letters indicate the target sequence for the gene; lowercase letters at 5′ or 3′ indicate the sticky ends to make the shRNA sequences successfully insert into the vector; lowercase letters in the middle of the sequence indicate the palindromic sequence to make the shRNA work.

Table S6. **Antibodies used in this study**

Antibody	Source	Catalog no.
PerCP anti-human CD45 antibody	BioLegend	368506
PerCP anti-human CD8a antibody	BioLegend	300922
FITC anti-human CD8a antibody	BioLegend	300906
Anti-human CD4/CD25 cocktail, APC, FITC	eBioscience	22-0425-71
Anti-human FOXP3 antibody, PE	eBioscience	12-4776-42/41
FITC anti-human HLA-DR	BioLegend	307604
PerCP/Cy5.5 anti-human CD33	BioLegend	366616
APC anti-mouse/human CD11b	BioLegend	101212
APC/Cy7 anti-human CD279 (PD-1) antibody	BioLegend	367416
PerCP/Cy5.5 anti-human CD366 (Tim-3) antibody	BioLegend	345016
PerCP/Cy5.5 anti-mouse CD45 antibody	BioLegend	103130
PE anti-mouse CD3 antibody	BioLegend	100206
FITC anti-mouse CD8a antibody	BioLegend	100706
PerCP/Cy5.5, anti-mouse CD4 antibody,	eBioscience	45-0042-82
CD25 Monoclonal antibody, PE	eBioscience	12-0251-83
FOXP3 monoclonal antibody, APC	eBioscience	17-5773-82
PE anti-mouse Ly-6G/Ly-6C (Gr-1) antibody	BioLegend	108408
PE anti-mouse F4/80 antibody	BioLegend	135206
APC anti-mouse IFN-γ antibody	BioLegend	505810
PE anti-mouse CD279 (PD-1) antibody	BioLegend	135206
APC anti-mouse CD366 (Tim-3) antibody	BioLegend	134008
PE annexin V	eBioscience	12-8102-69
PerCP/Cy5.5, 7-AAD	eBioscience	00-6993-42

Table S7. **Primers used for qRT-PCR and ChIP in this study**

Gene name	Forward	Reverse
hEHF	5′-TGCAGCATCTGAAGTGGAAC-3′	5′-AGGAAGGTGACTGGTGGTTG-3′
hTGFB1	5′-GCCACAGATCCCCTATTCAA-3′	5′-GTCTCCCGGCAAAAGGTAG-3′
hCSF1	5′-TAGCCACATGATTGGGAGTG-3′	5′-TATCTCTGAAGCGCATGGTG-3′
hCSF2	5′-GGCTAAAGTTCTCTGGAGGATG-3′	5′-CATCTCAGCAGCAGTGTCTCT-3′
hCSF3	5′-GTGCCACCTACAAGCTGTGC-3′	5′-AAAGGCCGCTATGGAGTTGG-3′
hVEGFA	5′-TTAAACGAACGTACTTGCAGATG-3′	5′-AGAGGTCTGGTTCCCGAAA-3′
hCOX2	5′-GCCTTCTCTAACCTCTCC-3′	5′-CTGATGCGTGAAGTGC-3′
hCCL2	5′-TCCCCAGACAVVCTGTTTTA-3′	5′-TCAAAACATCCCAGGGGTAG-3′
hCCL5	5′-CGCTGTCATCCTCATTGCT-3′	5′-ACACACTTGGCGGTTCTTTC-3′
hCXCL8	5′-GAGCACTCCATAAGGCACAA-3′	5′-AGCTGCAGAAATCAGGAAGG-3′
hIDO1	5′-ATGCAGACTGTGTCTTGGCA-3′	5′-GCGCCTTTAGCAAAGTGTCC-3′
hGAPDH	5′-GGGTTCCTATAAATACGGACTGC-3′	5′-CCATTTTGTCTACGGGACGA-3′
EHFChIP-TGFB1-1	5′-CCGCAAAGCCACAGCGCATC-3′	5′-TCGGCAGGGGGTTTTGAAGC-3′
EHFChIP-TGFB1-2	5′-GTCTGGTCCCCACCCATCCCT-3′	5′-CGGCCCACCACCCACGAAA-3′
EHFChIP-CSF2-1	5′-GCCCTATCTAAGTGTCTCCCA-3′	5′-TCCCTGGGCAGTCTGAATG-3′
EHFChIP-CSF2-2	5′-AAAACATCCTCCCCTCTACCA-3′	5′-AAGGTATCTGGCTCAAGCTG-3′

Table S8. **Sequence of the vectors for luciferase analysis**

Vector sequence
EHF-TGFB1-WT
5′-ggaaACGCGTcaaggcccatgatggttacctggggactggaggagcaatgggctgccctgacatggggtcatggaggaggataacacagagaggaaattcagcagaggtctgattagaagggccttgaatgttgaaga ggttggactttatactgagggcactggggagctatggaaggatccttagcaggggagtaacatggatttggaaagatcactttggctgctgtgtggggatagataagacggtgggagcctagaaaggaggctgggttggaaact ctgggacagaaacccagagaggaaaagactgggcctggggtctccagtgagtatcagggagtggggaatcagcaggagtctggtccccacccatccctccttttcccctctctctccttttcctgcaggctggccccggctc**catttc caggtg**tggtcccaggacagctttggccgctgccagcttgcaggctatggattttgccatgtgcccagtagcccgggcacccaccagctggcctgccccacgtggcggccccctgggcagttggcgagaacagttggcacgggct ttcgtgggtggtgggccgcagctgctgcatggggacaccatctacagtggggccgaccgctatcgcctgcacacagctgctggtggcaccgtgcacctggagatcggcctgctgctccgcaacttcgaccgctacggcgtggag tgctgagggactctgcctccaacgtcaccaccatccacaccccggacacccagtgatgggggaggatggcacagtggtcaagagcacagactctagagactgtcagagctgaccccagctaaggcatggcaccgcttctgtcct ttctaggacctcggggtccctctgggcccagtttccctatctgtaaattggggacagtaaatgtatggggtcgcagggtgttgagtgacaggaggctgcttagccacatgggaggtgctcagtaaaggagagcaattcttacaggtg tctgcctcctgacccttccatccttcaggtgtcctgttgcccccctcctcccactgacaccctccggaggcccccatgttgacagaccctcttctcctaccttgtttcccagcctgactctccttccgttctgggtcccctcctctggtcggc tcccctgtgtctcatccccggattaagccttctccgcctggtcctctttctctggtgacccacaccgcccgcaaagccacagcgcatctggatcacccgctttggtggcgcttggccgccaggaggcagcaccctgtttgcggggc ggagccggggtgcccgccccctttccccagggctgaagggaccccctcggagcccgcccacgcgagatgaggacggtggcccagccccccatgccctccccctgggggccgccccgctcccgccccgtg**cgcttcctg ggt**ggggccgggggcggcttcaaaacccctgccgacccagccggtccccgccgccgccgcCTCGAGttcc-3′
EHF-TGFB1-EBS1-mutation
5′-ggaaACGCGTcaaggcccatgatggttacctggggactggaggagcaatgggctgccctgacatggggtcatggaggaggataacacagagaggaaattcagcagaggtctgattagaagggccttgaatgttgaaga ggttggactttatactgagggcactggggagctatggaaggatccttagcaggggagtaacatggatttggaaagatcactttggctgctgtgtggggatagataagacggtgggagcctagaaaggaggctgggttggaaact ctgggacagaaacccagagaggaaaagactgggcctggggtctccagtgagtatcagggagtggggaatcagcaggagtctggtccccacccatccctccttttcccctctctctccttttcctgcaggctggccccggctc**catttc caggtg**tggtcccaggacagctttggccgctgccagcttgcaggctatggattttgccatgtgcccagtagcccgggcacccaccagctggcctgccccacgtggcggccccctgggcagttggcgagaacagttggcacgggct ttcgtgggtggtgggccgcagctgctgcatggggacaccatctacagtggggccgaccgctatcgcctgcacacagctgctggtggcaccgtgcacctggagatcggcctgctgctccgcaacttcgaccgctacggcgtggag tgctgagggactctgcctccaacgtcaccaccatccacaccccggacacccagtgatgggggaggatggcacagtggtcaagagcacagactctagagactgtcagagctgaccccagctaaggcatggcaccgcttctgtcct ttctaggacctcggggtccctctgggcccagtttccctatctgtaaattggggacagtaaatgtatggggtcgcagggtgttgagtgacaggaggctgcttagccacatgggaggtgctcagtaaaggagagcaattcttacaggtg tctgcctcctgacccttccatccttcaggtgtcctgttgcccccctcctcccactgacaccctccggaggcccccatgttgacagaccctcttctcctaccttgtttcccagcctgactctccttccgttctgggtcccctcctctggtcggc tcccctgtgtctcatccccggattaagccttctccgcctggtcctctttctctggtgacccacaccgcccgcaaagccacagcgcatctggatcacccgctttggtggcgcttggccgccaggaggcagcaccctgtttgcggggc ggagccggggtgcccgccccctttccccagggctgaagggaccccctcggagcccgcccacgcgagatgaggacggtggcccagccccccatgccctccccctgggggccgccccgctcccgccccgtg**ttttttttt ttt**ggggccgggggcggcttcaaaacccctgccgacccagccggtcccgccgccgccgcCTCGAGttcc-3′
EHF-TGFB1-EBS2-mutation
5′-ggaaACGCGTcaaggcccatgatggttacctggggactggaggagcaatgggctgccctgacatggggtcatggaggaggataacacagagaggaaattcagcagaggtctgattagaagggccttgaatgttgaaga ggttggactttatactgagggcactggggagctatggaaggatccttagcaggggagtaacatggatttggaaagatcactttggctgctgtgtggggatagataagacggtgggagcctagaaaggaggctgggttggaaact ctgggacagaaacccagagaggaaaagactgggcctggggtctccagtgagtatcagggagtggggaatcagcaggagtctggtccccacccatccctccttttcccctctctctccttttcctgcaggctggccccggctc**tttttt ttttttt**ggtcccaggacagctttggccgctgccagcttgcaggctatggattttgccatgtgcccagtagcccgggcacccaccagctggcctgccccacgtggcggccccctgggcagttggcgagaacagttggcacgggctttc gtgggtggtgggccgcagctgctgcatggggacaccatctacagtggggccgaccgctatcgcctgcacacagctgctggtggcaccgtgcacctggagatcggcctgctgctccgcaacttcgaccgctacggcgtggagtgc tgagggactctgcctccaacgtcaccaccatccacaccccggacacccagtgatgggggaggatggcacagtggtcaagagcacagactctagagactgtcagagctgaccccagctaaggcatggcaccgcttctgtcctttc taggacctcggggtccctctgggcccagtttccctatctgtaaattggggacagtaaatgtatggggtcgcagggtgttgagtgacaggaggctgcttagccacatgggaggtgctcagtaaaggagagcaattcttacaggtgtct gcctcctgacccttccatccttcaggtgtcctgttgcccccctcctcccactgacaccctccggaggcccccatgttgacagaccctcttctcctaccttgtttcccagcctgactctccttccgttctgggtcccctcctctggtcggctcc cctgtgtctcatccccggattaagccttctccgcctggtcctctttctctggtgacccacaccgcccgcaaagccacagcgcatctggatcacccgctttggtggcgcttggccgccaggaggcagcaccctgtttgcggggcgga gccggggtgcccgccccctttccccagggctgaagggaccccctcggagcccgcccacgcgagatgaggacggtggcccagccccccatgccctccccctgggggccgccccgctcccgccccgtg**cgcttcctg ggt**ggggccgggggcggcttcaaaacccctgccgacccagccggtcccgccgccgccgcCTCGAGttcc-3′
EHF-TGFB1- EBS1+2-mutation
5′-ggaaACGCGTcaaggcccatgatggttacctggggactggaggagcaatgggctgccctgacatggggtcatggaggaggataacacagagaggaaattcagcagaggtctgattagaagggccttgaatgttgaaga ggttggactttatactgagggcactggggagctatggaaggatccttagcaggggagtaacatggatttggaaagatcactttggctgctgtgtggggatagataagacggtgggagcctagaaaggaggctgggttggaaact ctgggacagaaacccagagaggaaaagactgggcctggggtctccagtgagtatcagggagtggggaatcagcaggagtctggtccccacccatccctccttttcccctctctctccttttcctgcaggctggccccggctc**tttttt ttttttt**ggtcccaggacagctttggccgctgccagcttgcaggctatggattttgccatgtgcccagtagcccgggcacccaccagctggcctgccccacgtggcggccc**ctg**ggcagttggcgagaacagttggcacgggctttc gtgggtggtgggccgcagctgctgcatggggacaccatctacagtggggccgaccgctatcgcctgcacacagctgctggtggcaccgtgcacctggagatcggcctgctgctccgcaacttcgaccgctacggcgtggagtgc tgagggactctgcctccaacgtcaccaccatccacaccccggacacccagtgatgggggaggatggcacagtggtcaagagcacagactctagagactgtcagagctgaccccagctaaggcatggcaccgcttctgtccttttc taggacctcggggtccctctgggcccagtttccctatctgtaaattggggacagtaaatgtatggggtcgcagggtgttgagtgacaggaggctgcttagccacatgggaggtgctcagtaaaggagagcaattcttacaggtgtct gcctcctgacccttccatccttcaggtgtcctgttgcccccctcctcccactgacaccctccggaggcccccatgttgacagaccctcttctcctaccttgtttcccagcctgactctccttccgttctgggtcccctcctctggtcggctcc cctgtgtctcatccccggattaagccttctccgcctggtcctctttctctggtgacccacaccgcccgcaaagccacagcgcatctggatcacccgctttggtggcgcttggccgccaggaggcagcaccctgtttgcggggcgga gccggggtgcccgccccctttccccagggctgaagggaccccctcggagcccgcccacgcgagatgaggacggtggcccagccccccatgccctccccctgggggccgccccgctcccgccccgtg**ttttttttttttt**ggg gccgggggcggcttcaaaacccctgccgacccagccggtcccgccgccgccgcCTCGAGttcc-3′
EHF-CSF2-WT
5′-ggaaACGCGTacagtggggtctggaggactaaggtttggtttctctatgcaaggtcagaaaaactcccacagtacagggaaactggccagggctgcagactcagaccacagtgctaaagccatgaactccacctgctctct gaaggctcgccaacctgagtccagcagaatgttctcgcttgtgtccaaccccactggtttaggctgaatcagcctctagggcccagaggcactgcacctggagtagggagcttctccagtatcagagtcaccttcagaggcctggag cctttcataaagcaggtaagaggactcaatagatgcatctgcatggaaaacatcctcccctctaccaggcacctgtatgtacaaccaatcacagcagcacacata**cacccagaaatg**ggcacgtgtgggcccacacccctttag ctatgaaacccaggcatggggcagcttgagccagatacctttgtgcaaacacaaactcgtgctgtcttctctgaactccattgtgaaaatcaaacacttgtcagcccctcaagagcctttagatttcctacttccacacttccacaga aaggcctctggagttgggggatgctggggttatgtaggaaattaagcctggagggccttgctggggaagccattgtccctgtacctgagatggatgcagccacagccctggagccagcctgaagctcctggtgtcttctgggggcta catataggagtgtagtccgaacctcagaggggcaaacctgctctgcagagggaatcaaggttcacataaccagagaggggagtcactcaggaaggtggctccagagccaagagtcagactctgggtcccgacttgacccagcca cacccctctgaagcttgctgagagtggctgcagtctcgctgctggatgtgcacatggtggtcattccctctgctcacaggggcagggtccccctactggactgaggttgcccctgctccaggtcctgggtgggagcccatgt gaactgtcagtgggcaggtctgtgagagctcccctcacactcaagtctctcacagtggccagagaagaggaaggctggagtcagaatgaggcaccagggcgggcatagcctgcccaaaggccctgggattacaggcaggatg gggagccctatctaagtgtctcccacgcccaccccagccattcca**ggccaggaagtc**caaactgtgcccctcagagggaggggcagcctcaggccattcagactgcccagggagggctggagagccctcaggaaggcgg gtgggtgggctgtcggttcttggaaaggttcattaatgaaaaccccaagcctgaccacctagggaaaaggctcaccgttcccatgtgtggctgataagggccaggagattccacagttcaggtagttcccccgcctccctggcatt ttgtggtcaccattaatcatttcctctgtgtatttaagagctcttttgccagtgagcccaCTCGAGttcc-3′

Table S8. **Sequence of the vectors for luciferase analysis (*Continued*)**

Vector sequence
EHF-CSF2-EBS1-mutation
5′-ggaaACGCGTacagtggggtctggaggactaaggtttggtttctctatgcaaggtcagaaaaactcccacagtacagggaaactggccagggctgcagactcagaccacagtgctaaagccatgaactccacctgctctct gaaggctcgccaacctgagtccagcagaatgttctcgcttgtgtccaaccccactggtttaggctgaatcagcctctagggcccagaggcactgcacctggagtagggagcttctccagtatcagagtcaccttcagaggcctggag ccttttataaagcaggtaagaggactcaatagatgcatctgcatggaaaacatcctcccctctaccaggcacctgtatgtacaaccaatcacagcagcacacata**cacccagaaatg**ggcacgtgtgggcccacacccctttag ctatgaaacccaggcatggggcagcttgagccagatacctgtgcaaacacaaactcgtgctgtcttctctgaactccattgtgaaaatcaaacacttgtcagcccctcaagagcctttagatttcctacttccacacttccacaga aaggcctctggagttgggggatgctggggttatgtaggaaattaagcctggagggccttgctggggaagccattgtccctgtacctgagatggatgcagccacagccctggagccagcctgaagctcctggtgtcttctgggggcta catataggagtgtagtccgaacctcagaggggcaaacctgctctgcagagggaatcaaggttcacataaccagagaggggagtcactcaggaaggtggctccagagccaagagtcagactctgggtcccgacttgacccagcca caccccctctgaagcttgctgagagtggctgcagtctcgctgctggatgtgcacatggtggtcattccctctgctcacaggggcaggggtccccccttactggactgaggttgcccctgctccaggtcctgggtgggagcccatgt gaactgtcagtggggcaggtctgtgagagctcccctcacactcaagtctctcacagtggccagagaagaggaaggctggagtcagaatgaggcaccagggcgggcatagcctgcccaaaggccctgggattacaggcaggatg gggagccctatctaagtgtctcccacgccccaccccagccattcca**ttttttttttttt**caaactgtgcccctcagagggaggggcagcctcaggcccattcagactgcccagggagggctggagagccctcaggaaggcgggtg ggtgggctgtcggttcttggaaaggttcattaatgaaaaccccaagcctgaccacctagggaaaaggctcaccgttcccatgtgtggctgataagggccaggagattccacagttcaggtagttcccccgcctccctggcattttg tggtcaccattaatcatttcctctgtgtatttaagagctcttttgccagtgagcccaCTCGAGttcc-3′
EHF-CSF2-EBS2-mutation
5′-ggaaACGCGTacagtggggtctggaggactaaggtttggtttctctatgcaaggtcagaaaaactcccacagtacagggaaactggccagggctgcagactcagaccacagtgctaaagccatgaactccacctgctctct gaaggctcgccaacctgagtccagcagaatgttctcgcttgtgtccaaccccactggtttaggctgaatcagcctctagggcccagaggcactgcacctggagtagggagcttctccagtatcagagtcaccttcagaggcctggag ccttttataaagcaggtaagaggactcaatagatgcatctgcatggaaaacatcctcccctctaccaggcacctgtatgtacaaccaatcacagcagcacacata**ttttttttttttt**ggcacgtgtgggcccacacccctttagcta tgaaacccaggcatggggcagcttgagccagatacctttgtgcaaacacaaactcgtgctgtcttctctgaactccattgtgaaaatcaaacacttgtcagcccctcaagagcctttagatttcctacttccacacttccacagaaag gcctctggagttgggggatgctggggttatgtaggaaattaagcctggagggccttgctggggaagccattgtccctgtacctgagatggatgcagccacagccctggagccagcctgaagctcctggtgtcttctgggggctacat ataggagtgtagtccgaacctcagaggggcaaacctgctctgcagagggaatcaaggttcacataaccagagaggggagtcactcaggaaggtggctccagagccaagagtcagactctgggtcccgacttgacccagccacac cccctctgaagcttgctgagagtggctgcagtctcgctgctggatgtgcacatggtggtcattccctctgctcacaggggcaggggtcccccttactggactgaggttgcccctgctccaggtcctgggtgggagcccatgtgaa ctgtcagtggggcaggtctgtgagagctcccctcacactcaagtctctcacagtggccagagaagaggaaggctggagtcagaatgaggcaccagggcgggcatagcctgcccaaaggccctgggattacaggcaggatgggg agccctatctaagtgtctcccacgccccaccccagccattcca**ggccaggaagtc**caaactgtgcccctcagagggaggggcagcctcaggcccattcagactgcccagggagggctggagagccctcaggaaggcgggtg ggtgggctgtcggttcttggaaaggttcattaatgaaaaccccaagcctgaccacctagggaaaaggctcaccgttcccatgtgtggctgataagggccaggagattccacagttcaggtagttcccccgcctccctggcattttg tggtcaccattaatcatttcctctgtgtatttaagagctcttttgccagtgagcccaCTCGAGttcc-3′
EHF-CSF2-EBS1+2-mutation
5′-ggaaACGCGTacagtggggtctggaggactaaggtttggtttctctatgcaaggtcagaaaaactcccacagtacagggaaactggccagggctgcagactcagaccacagtgctaaagccatgaactccacctgctctct gaaggctcgccaacctgagtccagcagaatgttctcgcttgtgtccaaccccactggtttaggctgaatcagcctctagggcccagaggcactgcacctggagtagggagcttctccagtatcagagtcaccttcagaggcctggag ccttttataaagcaggtaagaggactcaatagatgcatctgcatggaaaacatcctcccctctaccaggcacctgtatgtacaaccaatcacagcagcacacata**ttttttttttttt**ggcacgtgtgggcccacacccctttagcta tgaaacccaggcatggggcagcttgagccagatacctttgtgcaaacacaaactcgtgctgtcttctctgaactccattgtgaaaatcaaacacttgtcagcccctcaagagcctttagatttcctacttccacacttccacagaaag gcctctggagttgggggatgctggggttatgtaggaaattaagcctggagggccttgctggggaagccattgtccctgtacctgagatggatgcagccacagccctggagccagcctgaagctcctggtgtcttctgggggctacat ataggagtgtagtccgaacctcagaggggcaaacctgctctgcagagggaatcaaggttcacataaccagagaggggagtcactcaggaaggtggctccagagccaagagtcagactctgggtcccgacttgacccagccacac cccctctgaagcttgctgagagtggctgcagtctcgctgctggatgtgcacatggtggtcattccctctgctcacaggggcaggggtcccccttactggactgaggttgcccctgctccaggtcctgggtgggagcccatgtgaa ctgtcagtggggcaggtctgtgagagctcccctcacactcaagtctctcacagtggccagagaagaggaaggctggagtcagaatgaggcaccagggcgggcatagcctgcccaaaggccctgggattacaggcaggatgggg agccctatctaagtgtctcccacgccccaccccagccattcca**ttttttttttttt**caaactgtgcccctcagagggaggggcagcctcaggcccattcagactgcccagggagggctggagagccctcaggaaggcgggtgggt gggctgtcggttcttggaaaggttcattaatgaaaaccccaagcctgaccacctagggaaaaggctcaccgttcccatgtgtggctgataagggccaggagattccacagttcaggtagttcccccgcctccctggcattttgtgg tcaccattaatcatttcctctgtgtatttaagagctcttttgccagtgagcccaCTCGAGttcc-3′

Uppercase letters at 5′ and 3′ indicate the restriction enzyme cutting site added to the coding sequences of the gene; bolded letters indicate the WT or mutated sequences at ChIP-binding sites in the promoter of the gene. WT, wild type 2.